A Useful Approximation to Add up Contributions in Ray Based EM Propagation Algorithms

(Article begins on next page)

17 April 2024

Session 3AP
Poster Session 2

A New Non-paraxial Time-domain Method for Modeling Ultra Short Optical Pulses

Husain M. Masoudi[1, 2]

[1]Department of Electrical Engineering, King Fahd University of Petroleum and Minerals
Dhahran 31261, Saudi Arabia
[2]Electrical and Computer Engineering Department, Emerging Communications Technology Institute
University of Toronto, 10 King's College Rd. M5S 3G4, Ontario, Canada

Abstract— A new non-paraxial technique to model ultra short optical pulses has been proposed, implemented and verified. The technique uses rational complex coefficient approximation of Pade approximant $\sqrt{1+X} \approx \prod_{i=1}^{p} \left[(1 + a_i^p X) / (1 + b_i^p X) \right]$ to overcome the paraxial limitation. The aim of this technique is to model efficiently very short pulses in long optical structures. The implementation and the verification of the technique show excellent results in terms of accuracy, efficiency and stability where the traditional paraxial Time-Domain Beam Propagation Method failed to achieve [1]. The method is based on the idea of the paraxial TD-BPM, in which the wave equation is written as a one-way wave propagation equation along the direction of z while retaining the time variation as another axis down with the other transverse spatial dimensions that can be represented as

$$\frac{\partial^2 E}{\partial z^2} - 2jk\frac{\partial E}{\partial z} + \nabla_\perp^2 E + \left(n^2 k_o^2 - k^2\right) E - \frac{n^2}{c_o^2}\frac{\partial^2 E}{\partial \tau^2} - 2j\frac{n^2}{c_o}k_o\left(\frac{1}{c_o} - \frac{1}{v_g}\right)\frac{\partial E}{\partial \tau} = 0$$

where v_g is the pulse group velocity. This arrangement has the advantage of allowing the time window to follow the evolution of the pulse and hence minimizes the required computer resources. After factorizing the above equation into a forward and a backward operators, the one way wave equation can be written as [2]

$$E(z) = \exp\left(jk_o n_o z\right) \times \exp\left(-jk_o n_o \sqrt{1 + X z}\right) E(0)$$

We apply this technique to model ultra short optical pulse propagation using Finite Difference approach.

The figure shows a comparison between the present technique and the parabolic method for different initial ultra short pulse widths. The figure shows the divergence of the parabolic method
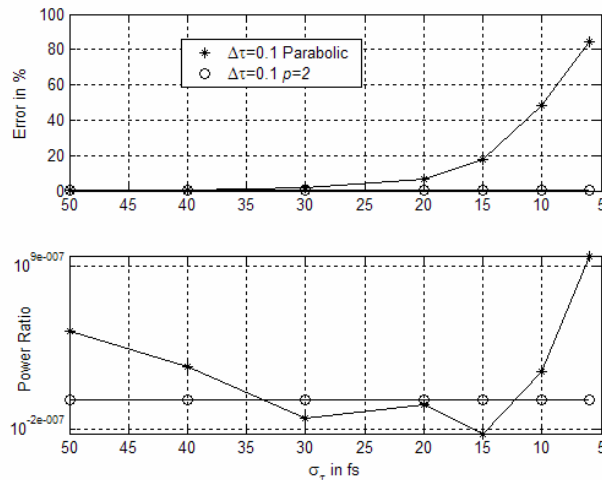
Figure 1: Comparison between the new technique and the parabolic Time Domain BPM for different initial ultra short pulse width. (Upper) The percentage maximum field error (Lower) The power ratio of the pulsed beam.

for ultra short pulse widths, where the error here is mostly associated with the paraxial approximation although very small time step was used. On the other hand, the present technique shows an outstanding performance even for ultra small optical pulse widths. Again from the figure one also notices the strong stability of the present technique compared with the parabolic counterpart.

ACKNOWLEDGMENT

REFERENCES

1. Masoudi, H. M., M. A. AlSunaidi, and J. M. Arnold, "Efficient time-domain beam propagation method for modelling integrated optical devices," *J. of Lightwave Technology*, Vol. 19, No. 5, 759–771, May 2001.
2. Masoudi, H. M., "A stable time-domain beam propagation method for modelling ultra short optical pulses," to appear in *IEEE Phtonics Technology Letters*, 2007.

A Novel Approach to Model Linear and Nonlinear Dispersion with ADE-FDTD

M. Ammann[1], **S. Schild**[1], **N. Chavannes**[2], **and N. Kuster**[1]

[1]Foundation for Research on Information Technologies in Society (IT'IS), ETHZ, Switzerland
[2]Schmid & Partner Engineering AG, 8004 Zurich, Switzerland

Abstract— Emerging applications in photonics in general and of metamaterials in particular involve media with frequency and intensity dependent polarisations. A novel finite-difference time-domain (FDTD) algorithm for arbitrary dispersive media (ADM) allows to model materials with linear multipole Drude- and Lorentz dispersion as well as Kerr-Effect and Raman-Scattering. The ADM algorithm is faster than any previously reported solution (e.g., [1]) while providing full modularity allowing to model every combination of the mentioned phenomena. Moreover, it has proven stability conditions for every effect as well as the used fixed-point iteration.

Methodology

Consider the FDTD expression of Ampere's law

$$\nabla \wedge \mathbf{H^{n+\frac{1}{2}}} = \epsilon_0 \epsilon_\infty \frac{\mathbf{E^{n+1}} - \mathbf{E^n}}{\mathbf{\Delta t}} + \frac{\mathbf{P_{tot}^{n+1}} - \mathbf{P_{tot}^n}}{\mathbf{\Delta t}} + \sigma \frac{\mathbf{E^{n+1}} + \mathbf{E^n}}{\mathbf{2}} \tag{1}$$

where in the presence of Drude- and Lorentz-Poles, Kerr-Effect and Raman-Scattering the finite-difference formulation of the total polarisation $\mathbf{P_{tot}}$ is given by

$$\mathbf{P_{tot}^{n+1}} - \mathbf{P_{tot}^n} = \sum_{\mathbf{l,d=1}}^{\mathbf{L,D}} \left(\mathbf{P_{l,d}^{n+1}} - \mathbf{P_{l,d}^n} \right) + \epsilon_0 \left(\mathbf{R^{n+1}E^{n+1}} - \mathbf{R^nE^n} \right) + \alpha \left(|\mathbf{E^{n+1}}|^\mathbf{2}\mathbf{E^{n+1}} - |\mathbf{E^n}|^\mathbf{2}\mathbf{E^n} \right). \tag{2}$$

The last term, being the contribution from the Kerr-effect, renders the finite-difference fomulation of Ampere's Law non-linear in $\mathbf{E^{n+1}}$. To avoid the costly matrix inversion in each Newtoniteration and to preserve modularity, the new variable

$$I^n \doteq |\mathbf{E^n}|^\mathbf{2} \tag{3}$$

is introduced to gain linearity in $\mathbf{E^{n+1}}$. It is shown that the update equation of I^n is badly conditioned for the Newton-method but can be solved efficiently through a fixed-point iteration with guaranteed convergence. Despite the fixed-point iteration converging slower than the Newton-iteration, the new formulation is by orders of magnitude faster as far less computations per iteration are required.

Results

The algorithm is integrated into the EM simulation patform SEMCAD X. The modularity allows to use conventional solvers including hardware accelration solutions to solve for the linear part of the update equations and to add the nonlinear contributions where necessary.

The *ADM* algorithm is shown to be significantly faster than the approach presented in [1] while its modularity and speed have proven to allow efficient integration into existing FDTD software. The algorithm was implemented and tested in full 3D including simulations of metamaterials with nonlinear dispersion, successfully simulating effects such as EM-cloaking and gap-solitons.

REFERENCES

1. Greene, J. H. and A. Taflove, "General vector auxiliary differential equation finite-difference time-domain method for nonlinear optics," *Opt. Express*, Vol. 14, No. 18, 8305–8310, 2006.

Interference Calculation for ATSC System against Interference from ISDB-T System Using Computational Simulation

Sung Woong Choi[1], **Tae Jin Jung**[2], **Wang Rok Oh**[3], **and Heon Jin Hong**[1]

[1]Radio & Broadcasting Technology Lab., ETRI, Korea
[2]Department of Electronic & Computer Engineering, Chonnam National University, Korea
[3]Division of Electrical & Computer Engineering, Chungnam National University, Korea

Abstract— Until now, it is general that the field test data are used for setting up the PR between the broadcasting systems. But it needs much time and cost order collect and analyze the field test data. Therefore, by drawing method for setting up the PR based on the computational simulation, it it easy to calculate the PR about the corresponding system.

In this paper, we proposed the method for calculating the PR of the ATSC broadcasting system from the ISDT-T broadcasting system through the computational experiment. For this, the transmitter/receiver of the ATSC system and transmitter of the ISDB-T system were modeled. By integrating those, the computational simulator for setting up the PR of the ATSC system from the ISDB-T system was implemented. The ATSC TV signal was regarded as the desired one and the ISDB-T TV signal was regarded as the interfering one. In order to simplify the simulation complexity, it modeled sending/receiving signals of the IF band instead of those of the RF band. It is assumed the channel modeling one considered received signal and there's no AWGN noise.

Feasibility of Defect Detection in Concrete Structures via Ultrasonic Investigation

A. Musolino, **M. Raugi**, **M. Tucci**, and **F. Turcu**

Dipartimento di Sistemi Elettrici e Automazione, Via Diotisalvi, Pisa 2 56126, Italy

Abstract— In this paper we investigate the feasibility of a diagnostic method for the Non Destructive Test (NDT) of concrete structure based on the ultrasonic wave propagation.

The techniques based on ultrasounds have been introduced in the non destructive analysis in different engineering fields. In particular, in the case of plants with systems of pipes, ultrasonic waves, guided by the walls of the pipes themselves, have been used. The presence of a defect in the structure produces a reflected wave that can be detected by properly positioned sensors. The analysis of the waveforms of the sensor allows the localisation of the defect.

The diagnostic system MsM 2020 is available at the Department of Electrical System and Automation of the University of Pisa. It is based on a magnetostrictive transducer and has been used to generate the propagation of elastic waves in guiding tubular structures in order to perform the inspection if metallic pipes. The system is also able to stimulate planar structures when a properly designed set of transducer is used.

In order to asses the validity of the method we performed a number of numerical analysis on a sample structure shown in Fig. 1. The transducer is able to impose an assigned displacement along the x-direction to a rectangular portion of the surface of the slab. The waveform of this imposed displacement is shown in Fig. 2.

The displacements the points belonging to the face of the slab where the transducer is located are shown at different instant in the Figs. 3–5. Fig. 6 shows the waveform in the point A and B as indicated in Fig. 1.

The obtained results show the feasibility of the proposed method also in the examined example where the dimensions of the defect are smaller than the wavelength. The maps of the displacements show that the defect acts as a secondary source that superimposes his effects to those of the transducer used to excite the structure. The analysis of the waves that originate from this secondary source may be used to determine the position of the source itself.

Figure 1: Sample geometry.

Figure 2: Displacement imposed by the transducer.

Figure 3: X-displacement at 0.6 ms.

Figure 4: X-displacement at 0.72 ms.

Figure 5: Z-displacement at 0.6 ms.

Figure 6: X displacement at point A and B.

Localisation of Defects in Concrete Structures via the Cross Power Spectrum Phase

A. Musolino[1], M. Raugi[1], F. Turcu[1], R. Parisi[2], A. Uncini[2], A. Cirillo[2]

[1]Dipartimento di Sistemi Eletrici e Automazione, Università di Pisa, Via Diotisalvi, Pisa 2 56126, Italy
[2]INFOCOM Department, University of Rome "La Sapienza", Via Eudossiana 18, Rome 00184, Italy

Abstract— The ultrasonic test of masonry is a technique of current use that allows the inspection of large non accessible portions of buildings. The physical principle is based on the propagation of elastic waves in a guiding structure that is constituted by the volume under inspection. In a homogeneous indefinite medium the elastic waves propagate outward from the source. The ultrasonic waveforms commonly used in the tests are characterized by a frequency range bounded below by 20 kHz. The upper limit depends on the dimension of the masonry components that have to be smaller of the wavelength corresponding to the highest frequency. The use of frequencies greater than 1 MHz is quite rare. Since gaseous media do not transmit such waves, they are used to identify micro-cracks that are able to reflect the wave's front if their dimensions are comparable with the wavelength; the higher are the frequencies the smaller are the defects that can be detected. The frequency cannot be arbitrarily increased as the ultrasonic signal is highly attenuated when its wavelength is comparable with the dimensions of the masonry components because of the presence of a huge number of reflections caused by the masonry components. Essentially the propagation medium cannot be considered as homogeneous and as a consequence the discrimination between defects and masonry component based on the wave front reflection is no longer possible.

While the reflection due to the masonry component can be avoided by using properly chosen (low enough) frequencies, the reflection due to the boundaries of the structure are always present. These reflections interfere with those produced by internal defects and make it the recognition of the components due to the defect a very difficult task. In this situation the use of multiple sensors might help in effectively localizing the internal defects.

Array processing has become a very popular discipline in many fields. Its success is motivated by the fact that combined use of spatial and temporal information allows to overcome the limitations of many practical information processing systems. Array processing techniques are typically employed to localize the sources emitting the observed signals. Typical applications can be found in radars, communications and acoustic signal processing.

In the problem under consideration, an array of sensors is deployed on the surface of the structure under exam to sense the ultrasonic field originated by the transducers. The ultrasonic field in the masonry structure is due to the superposition of waves emitted by transducers and those reflected by boundaries and internal defects. In particular, defects can be treated as *secondary sources*, whose position can be estimated by proper processing of acquired signals.

A number of techniques are available. In particular, source localization can be performed by a two step strategy. In the first step a set of relative time differences of arrival (TDOA) between pairs of sensor signals are estimated. Usually the well-known generalized crosscorrelation (GCC) is employed [1]. In the second step the source position is estimated by exploiting the derived TDOAs according to some specified strategy (e.g., by geometrical triangulation). The presence of reflections yields multiple peaks in the GCC function; proper strategies should be then devised in order to discriminate among peaks due to primary and secondary sources [2]. In particular the GCC function (or its frequency counterpart, called Cross Power Spectrum, CPS) can be exploited to derive an acoustic 3D map of the concrete structure [3]. In practice, a 3D grid is considered which contains the structure. A weighting function derived from the CPS is computed for each node of the grid in order to estimate the probability that a source (primary or secondary) is located in it. Since the positions of primary sources (the transducers) are known, this method allows to detect and localize the internal defects of the structure.

In particular in this work a novel weighting function has been introduced, in order to improve the robustness of the localization task. The proposed approach is based on selection of the most significant peaks each GCC, whose position is exploited to build a weighting functional based on the superposition of gaussian distributions. The proposed algorithm has been tested on simulated data. Preliminary results confirm the superiority of the proposed solution with respect to existing approaches in terms of localization accuracy.

REFERENCES

1. Knapp, C. H. and G. C. Carter, "The generalized correlation method for estimation of time delay," *IEEE Trans. on Acoust., Speech and Signal Processing*, Vol. 24, No. 4, Aug. 1976.
2. Parisi, R., A. Cirillo, M. Panella, and A. Uncini, "Source localization in reverberant environments by consistent peak selection," accepted for publication at *2007 IEEE Int. Conf. on Acoustics, Speech and Signal Processing*, Honolulu, Hawaii, USA, April 15–20, 2007.
3. Mungamuru, B. and P. Aarabi, "Enhanced sound localization," *IEEE Transactions on Systems, Man and Cybernetics*, Part B, Vol. 34, Issue 3, 1526–1540, June 2004.

Microwave Phase Interferometry for Nondestructive Testing in Industry

Ondrej Zak, **Jan Vrba**, **and Marika Pourova**

Department of Electromagnetic Field, FEE, CTU in Prague, Czech Republic

Abstract— In the paper contactless method for measurement of properties of constructional and machine material is dealt. It discuss phase microwave interferometry. We can determine e.g., moisture of material constructional and inner structure of material etc. via this method. Method is realized in a frequency range from 1 GHz to 8 GHz.

At present monitoring is currently implemented by a variety of sensors, such as network of optical targets installed over the structure, strain gauges to measure deformations, collimation nets to measure displacements, inclinometers to measure rotations. Such sensors are accurate and reliable, but require contact with the structure to be surveyed, and information is local to the specific point of the sensor position. In a number of situations, moreover, placing of sensors on the structure is not possible or is too time consuming. Calibers are used in measurement of definite dimensions, which are very expensive.

Therefore the method of microwave phase interferometry is developed. This method is contactless method for measurement i.e., moisture masonry, warping object or finding inner inhomogeneous in various build of material. We can minimize the costs of place and time for compile of measured date.

This method is used for detecting defects of optic transparent materials. But wavelength of light is manifold smaller than wavelength in microwave spectrum that is why we can't inquired into material helped by optic, which they are not optic transparent.

Principle of method is to measure face of equiphase surface unknown microwave field, so that unknown field interfere with reference field and we carry out scalar measurement of electrical field strength in single points of interferential field. When we use for measurement matrix decoder, we can carry out measurement in short interval. We can determine phase inquiry field from measured values of electrical strength field in single points, so that we change phase of reference field known for style. Then we calculate phase from measured values helped by known algorithms. Algorithms used for evaluation are implied from optic spectrum.

A Signal Explanation for the Electromagnetic Induction Law

S. L. Vesely[1] and A. A. Vesely[2]

[1]I.T.B. - C.N.R., via Fratelli Cervi 93, Segrate (MI) I-20090, Italy
[2]via L. Anelli 13, Milano 20122, Italy

Abstract— Today people consider the law of electromagnetic induction a consequence of the Lorentz force, the basic force in electrodynamics. As electromagnetism has merged with the latter theory, it does not seem reasonable to look for explanations that do not refer to electrodynamics.

Indeed, one reason to look for an alternative explanation is that, according to the equation, the microscopic Lorentz force that a magnet exercises on an elementary charge depends further only on their relative motion, and therefore the equation means as well that electricity can be transduced directly and independently of the system size into a mechanical effect. Though this is quite true of all electric motors, nevertheless the macroscopic approach to electromagnetic induction sticks to statistical mechanics, and explains the transient via lack of coherence between microscopic features or energy dissipation and associated heat.

Since the transitory aspect of the electric response is difficult to handle adhering to dynamic principles only, an explanation is called for as to why dissipation may occur. It can be understood that some form of friction stops the effect, once generated, from perpetuating. But if replacing the magnet with another electric winding has the same effect, it cannot be easily seen why it is generated with those characteristics both on switching on and on switching off the current. In fact J. Clerk Maxwell himself based his mechanical explanation of electromagnetic induction on idle wheels.

But as it is not truly necessary to provide a mechanics based approach for electricity, he finally summed up the effect called "electromagnetic induction" in one of a system of four fundamental equations, linking the variation of induction by the magnet to the electric current in a way that mathematically couples the equations. That development had a consistent mathematical meaning. However it was not also deemed a physical explanation.

Today to the plain description of facts, people prefer to confer reality on electric and magnetic fields, mathematical solutions to the whole equation system. Therefore the fields are considered as physical quantities, which means in the end that there is a prescribed method to measure **E** and **B** (in a vacuum). The operational interpretation, being an alternative interpretation of the system of equations, in particular does not explain electromagnetic induction.

Now Maxwell's electromagnetic induction equation exactly parallels the observed fact, which shows that the (relative) movement of a magnet through an electric coil is seen at the coil terminals as an electric transient, and that one can obtain the same kind of electric signal by substituting a linked inductor coil for the magnet.

Perhaps we will be able to understand the transient response of an electric winding on a purely electrical basis, i.e., starting from the analogous effect for a condenser. When a Leyden jar is electrically charged, touching it, there can be a number of shocks until discharge is reached. In this case it is as if the jar is not suddenly discharged, while transient electricity manifests itself. In the same way, when the electromagnetic induction transient ceases, simply no more signal is detected. Vice versa the signal is detected only when some coupling is mismatched. In fact a tuned resonance coupling within a system does not by itself entail any energy transfer, but an external load does.

According to the interpretation that we wish to suggest here, the descriptive induction equation written by Maxwell just tells that, under conditions of perfectly tuned resonance, that is, under steady conditions, there is no signal that a coupling may be present within an electric system. But the signal manifests as soon as resonance is spoiled. As is known, maximum transfer to a receiver occurs under matched conditions. It could be said that the principle of conservation of energy expresses the same concept. But we do not think so, because our explanation does not concern useful power transfer in electro-mechanics, but only the linear case contemplated by the induction equation.

Analytical Solutions to the Applicators for Microwave Textile Drying by Means of Zigzag Method

M. Pourová and J. Vrba

Department of Electromagnetic Field, Faculty of Electrical Engineering, Czech Technical University
Technická 2, 166 27 Prague 6, Czech Republic

Abstract— In this contribution we would like to describe the analytical method for solving microwave applicators for drying of textile materials, which is based on the solving transfer characteristics of waveguide with discontinuities.

We have designed two types of applicators, which we use for testing. The first applicator is derived from the Fabry-Perrot resonator, which is open type resonator. Whole system works at frequency 2.45 GHz and uses magnetron, which generates power 700 W. This machine is intended for the drying at factory production of fabrics. The second one is waveguide type applicator, which is waveguide with a longitudinal slot in wider side of waveguide. This slot is situated in the middle of this side, because maximum of electric field strength is here. Waveguide proportions were designed so that only dominant mode TE_{10} could propagate inside the waveguide at the working frequency 2.45 GHz.

We analyzed drying system with the analytical method. This method is based on the solving transfer characteristics of waveguide with discontinuities. We can describe the wet textile as discontinuity by means of three quantities: the size of reflection coefficient $|\rho|$, its phase angle φ and phase angle ψ of transmission coefficient τ. The size of the transmission coefficient is defined by known relation $\tau\tau^* = 1 - |\rho|^2$ which results from the principle of conservation of energy.

We created diagram of EM waves inside this structure and reached the resulting expression, which is used for calculation of electric field strength in the plane of drying textile. This quantity depends on electrical characteristics of wet textile such as permittivity and loss factor. Measurements of these dielectric properties for the coburg is complicated and this method makes it possible to solve our problem with dielectric parameters. We can also describe the absorbed power in the textile in dependence on the dielectric properties.

The results of this method are very good corresponding with simulations and experimental measurements.

Broadband Leaky-wave Antenna Fed with Composite Right/Left Handed Transmission Line

Y. Miyama[1], T. Nishikawa[1], K. Wakino[1], Y.-D. Lin[2], and T. Kitazawa[1]

[1]Department of Electrical & Electronic Engineering, Ritsumeikan University, Japan
[2]Institute of Communication Engineering, National Chial Tung University, Taiwan, R. O. C.

Abstract— The broadband planar leaky-wave antenna fed with the composite right/left handed (CRLH) transmission line is presented. Tapered planar leaky-wave antenna element is designed based on the EM simulation for the broadband applications. The balanced feeding lines with 180-degree phase difference required for the selective excitation of odd leaky mode to the strip conductor is realized by inserting the section of CRLH in one branch of the feeding transmission lines. CRLH section is designed by using FEM simulator and composed with commodity chip capacitor and inductor in the market. Leaky-wave antenna system consisted of the tapered antenna element and CRLH feeder is designed and fabricated on commercially available high frequency substrate. Measured return loss is less than $-9.5\,\text{dB}$ over the wide frequency range more than $3.1\,\text{GHz}$. The measured radiation patterns show the familiar feature of the leaky-wave antennas.
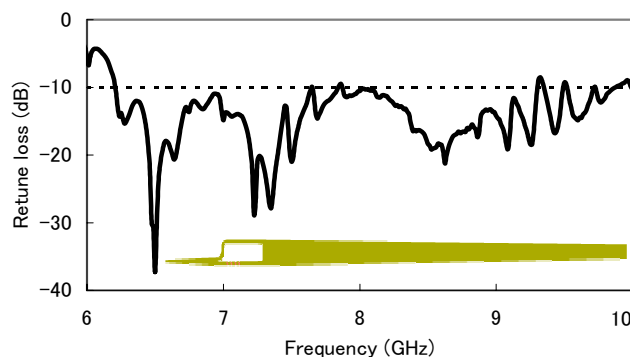
Figure 1: Measured retune loss frequency characteristics of leaky-wave antenna system.

Modeling and Simulation of UWB Signal for Indoor Radio Channels

Je-Sung Ahn[1], Seo Yu Jung[1], Deock-Ho Ha[1], Young-Hwan Lee[2], and Dong-Won Jang[2]

[1]Department of Telecommunication Engineering, Pukyong National University, Busan, Korea
[2]Technical Regulation Research Team, ETRI, Daejeon, Korea

Abstract— In this paper, we describe the indoor radio channel characteristic of Ultra-wideband signals by computer simulation. To analyze the propagation characteristic of UWB radio signals, we used the parameter proposed by IEEE P802.15 WPANs in 2003. From the simulation analysis, it can be clearly seen that the UWB signals generated by insufficient time intervals should be encountered to intersymbol interference due to mean excess delay and RMS delay. In addition, it was found that the total usable number of receiver depends on the number of significant paths within 10 dB of peak, or depends on the number of significant paths capturing 85% higher level for the total energy.

Introduction: In this paper, we analyzed the propagation characteristic and implemented the channel simulator for the UWB system parameters. The impulse response, average power delay profile and the number of multipath components are studied. From these data, we studied and analyzed the radio propagation characteristic of UWB band representing path loss model. In general, many models are available in the literature for predictions and simulation of indoor channel. To investigate the radio channel characteristic, we used channel environments reported in IEEE 802.15-02/294SG3a and adopted their model parameters [1].

UWB Channel Model and Channel Simulator: To analyze the system performance of PHY, a multipath channel model is proposed by IEEE 802.15 Study Group 3a High Rate WPAN [2]. Based on the clustering phenomenon observed in several channel measurements, they proposed UWB channel model derived from the Saleh-Valenzuela model with a couple of slight modification [3]. In this paper, we implemented a channel simulator using by this model to analyze the propagation characteristic of UWB indoor radio channel. Tab1e 1 shows the characteristic of channel parameters. Figure 1 shows the flowchart of the simulation procedure.

Model parameters	CM1	CM2	CM3	CM4
Λ (1/nsec)	0.0233	0.4	0.0667	0.0667
λ (1/nsec)	3.5	1	3	3
Γ	7.1	5.2	14.00	24.00
γ	4.3	6.7	7.9	12
σ_1 (dB)	3.3941	3.3941	3.3941	3.3941
σ_2 (dB)	3.3941	3.3941	3.3941	3.3941
σ_x (dB)	3.3941	3.3941	3.3941	3.3941
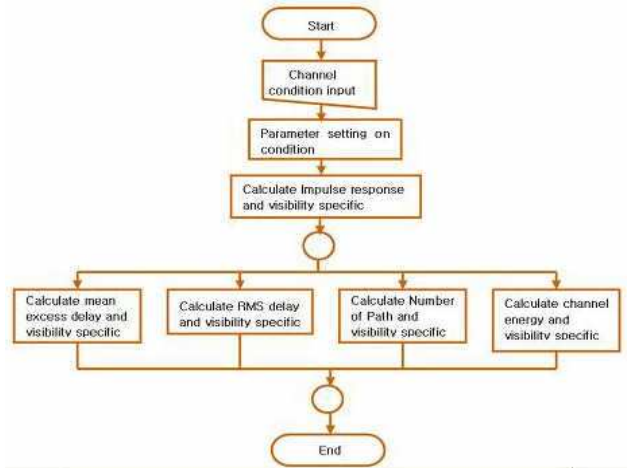
Table 1: Parameter characteristic for CM1-CM4.

Figure 1: Flowchart of the UWB channel simulator.

Simulation Results: Figure 2 shows the mean excess delay for each channel. The red line in the Figure 2 indicates the average value for each channel model. The average time which signal arrives to the transmitter from receiver is 5.0 nsec for CM1, 9.9 nsec for CM2, 15.9 nsec for CM3, 30.1 nsec for CM4, respectively. This means that the UWB time signal having insufficient time intervals can be affected by intersymbol interference, because the 500 MHz frequency bandwidth indicates 2 nsec time spread. The summery of simulation results are represented in Table 2.

Concluding Remarks: From this study, it can be clearly seen that the UWB signals generated by insufficient time intervals should be encountered to intersymbol interference due to mean excess delay and RMS delay. In addition, it was found that the total usable number of receiver depends on the number of significant paths within 10 dB of peak, or depends on the number of

CM1, CM2, CM3, CM4 Mean Excess Delay
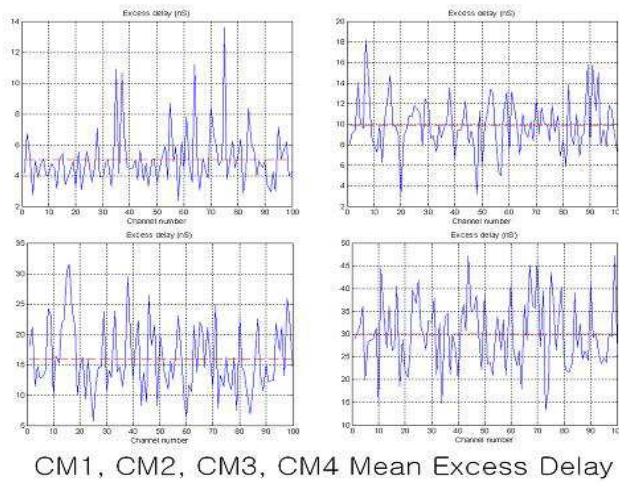
Figure 2: Mean excess delay for each CM1-CM4.

Channel Characteristics	CM1	CM2	CM3	CM4
Mean excess delay (nsec)	5.0	9.9	15.9	30.1
RMS delay (nsec)	5	8	15	25
NP(10dB)	12.5	15.3	24.9	41.2
NP(85%)	20.8	33.9	64.7	123.3
Channel energy mean(dB)	-0.4	-0.5	0.0	0.3
Channel energy std.(dB)	2.9	3.1	3.1	2.7

Table 2: Results of channel characteristic.

significant paths capturing 85% higher level for the total energy. Therefore, we recommend that the UWB system such as DS-CDMA, MB-OFDM must be designed by considering the complex of receiver in NLOS or LOS environments. And also, the UWB channel simulator developed in this research can be used in analyzing the channel interference.

REFERENCES

1. Pendergrass, M., "Empirically based statistical ultra-wideband channel model," *IEEE P802.15- 02/240-SG3a*.
2. Foerster, J. and Q. Li, "Channel modeling contribution from Intel," *IEEE P802.15-02/490r-SG3a*, February 2003.
3. Saleh, A. and R. Valenzuela, "A statistical model for indoor multipath propagation," *IEEE Journal of SAC.*, Vol. SAC-5, No. 2, 128–137, February 1987.
4. FCC, "Revision of part 15 of the commission's rules regarding ultra-wideband transmission systems," First Report and Order, ET Docket 98–153, Feb. 2002.

Modal Analysis of Miniature Microstrip Patch Antennas Based on Fractal Geometry

P. Hazdra and M. Mazanek

Department of Electromagnetic Field, FEE, Czech Technical University in Prague
Technicka 2, Prague 166 27, Czech Republic

Abstract— The paper deal with the fractal microstrip patch antennas with specific properties based on rearrangement of current densities on their surface by means of special fractal geometrical modifications. Description of physical behavior via surface current distribution and radiation properties are summarized. Different modal analysis approaches (cavity model and the Theory of characteristic modes) have been used for the simulations.

Meandering of surface current paths associated with the operational modes is effective way for lowering resonance frequency or decreasing antenna dimension when the resonant frequency is maintained. Plenty of configurations have been proposed based on introducing slot and notch types of perturbation elements (PE) that force the surface currents to flow around PEs. These configurations have a general drawback in increasing of cross-polar level and decreasing impedance bandwidth due to the resonance behaviour of highly geometrically modified patches. Advantage of further presented set of fractally modified patches with fixed outer sizes is relatively small cross-polar level compared to the patches designed by standard techniques using slot and notche types of PEs.

Among others, study of so-called Inverted Koch Square Patch with indentation angle 85° and of iteration order 3, is presented. It has been found that a special current distribution of fundamental mode causes significant lowering of resonant frequency compared to canonical structures. To gain deeper insight into properties of the proposed structures, well-known cavity model and the theory of characteristic modes (TCM), which both allows perform modal analysis of structures independent of its feed configuration, have been used. The patch shape is generated by the L-System fractal generator.

Algorithm for Noise Reduction in Output Signal of Race-track Core Fluxgate

M. Butta[1], **P. Ripka**[1], **and J. Kubík**[1,2]

[1]Department of Measurement, Czech Technical University, Technická 2, Praha 166 27, Czech Republic
[2]Tyndall National Institute/MAI, Lee Maltings, Prospect Row, Cork, Ireland

Abstract— We present a novel algorithm for noise reduction in fluxgate sensors [1].

Noise measurements have been performed on the output signal of the race-track core PCB fluxgate sensor [2] inserted into a six-layer magnetic shielding. The output signal has been conditioned using a low noise amplifier Stanford Research SR560, then sampled with high speed digitizer NI 5911. Proper amplifying gain and high resolution (18 bits) of the digitizer gave as a result the possibility to properly measure the even harmonics, even if buried in higher amplitude signal at odd harmonics. This method, based on the sampling of the signal, allowed us to measure all the even harmonics simultaneously. Similar measurement with conventional lock-in amplifier would be of excessive complexity. The resulting noise on all even harmonics was then subjedcted to statistical analysis: a strict correlation between them is clearly shown from their variations in time [3]. The algorithm for noise reduction is proposed based on this key feature of the noise. While the sensitivity at the even harmonics is rather different, the noise is quite similar both in average rms value and varying part, which has been shown to be strictly correlated. The proposed algorithm is based on the proper linear combination of even harmonics in order to obtain suppression of the noise, even with the drawback of a reduction in sensitivity. Detailed analysis is finally shown for the achievement of optimum t performance for both noise reduction and sensitivity.
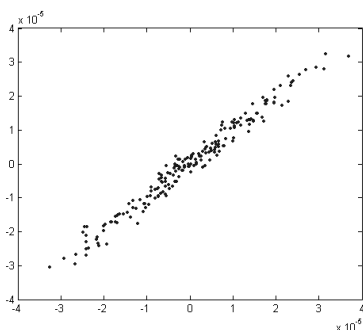
Figure 1: Correlation between 2nd and 4th harmonic.
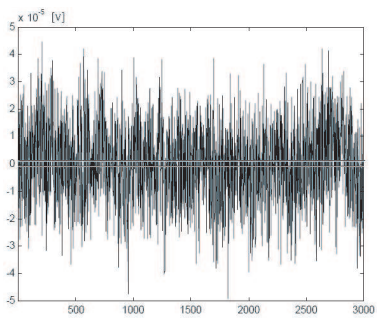
Figure 2: Noise at 2nd Harmonic vs period.
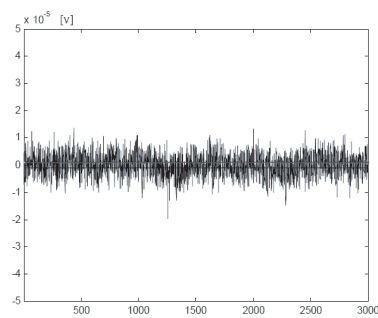
Figure 3: Noise at output signal of the algorithm vs period.

REFERENCES

1. *Magnetic Sensors and Magnetometers*, Pavel Ripka (ed.), 78–79, Artech House, 2001.
2. Kubík J., L. Pavel, and P. Ripka, "PCB racetrack fluxgate sensor with improved temperature stability," *Sensors and Actuators A*, Vol. 130, 184–188, 2006.
3. Butta, M., "An innovative algorithm for noise reduction in a fluxgate output signal," MSc Thesis work in Electrical Engineering, Politecnico di Milano, 2005.

Polarization-dependent Diffraction of Cholesteric Liquid Crystal Grating with Silver Nanoparticles

I.-Min Jiang[1], **Ming-Shan Tsai**[2], **Wen-Chi Hung**[3], **and Wood-Hi Cheng**[3]

[1]Department of Physics, National Sun Yat-sen University, Kaohsiung 804, Taiwan, R. O. C.
[2]Department of Applied Physics, National Chiayi University, Chiayi 600, Taiwan, R. O. C.
[3]Institute of Electro-Optical Engineering, National Sun Yat-sen University
Kaohsiung 804, Taiwan, R. O. C.

Abstract— The polarization-dependent diffraction of cholesteric liquid crystal (CLC) grating was demonstrated in this study. One of ITO glass plates of the CLC grating cell was covered by silver nanoparticles. The CLC grating was probed by the polarized monochromatic beam, and the wavelength was scanned from 450 nm to 700 nm. While the polarization angle of the incident beam was rotated from 0 to 90, the blue-shift phenomenon was observed in the diffraction spectrum. The novel blue-shift phenomenon could cause by the periodic variation of the localized surface plasmon excitation emerged from silver nonoparticles in the CLC grating. The polarization dependent property enables a flexible modulation in the diffraction efficiency that offers potential applications in the switch devices.

ACKNOWLEDGMENT

A Useful Approximation to Add up Contributions in Ray Based EM Propagation Algorithms

Marco Allegretti, **Luca Coppo**, and **Giovanni Perona**

Electronic Department, Politecnico di Torino
C.so Duca degli Abruzzi 24, Torino 10129, Italy

Abstract— In last years ICTs required a huge development of wireless communication channels. The growth of wireless devices distribution induces channels to carry a large amount of data, so leading transmission frequency to increase. At the same time respecting environmental shock criteria requires the transmission power to be as low as possible. In such context, an optimized wireless network plan is the best way to lower transmission power and optimize radio coverages.

Electromagnetic (EM) propagation simulation represents a good way to predict the distribution of the electric field avoiding in-place field measures. Automated wireless network design routines can include simulation results as a feedback to improve network parameters until project constraints have been satisfied. Despite modern electronic calculators have reached very high levels of computation strength, EM propagation simulation requires punctual evaluation of the field yielding simulation algorithms more complex. Hypothesis of high frequency (short wavelength) allow simulation routines to use simplified deterministic ray-based propagation models such as Ray-Tracing and Ray-Launching algorithms.

In ray-based algorithms the punctual value of the electric field is function of contributes of each ray reaching the specified point. Considering a perfect system geometry, the electric field may be evaluated as a magnitude and phase sum of all the contributions given by incident rays. This solution cannot be applied in real environments, where high frequency ($> 2\,\mathrm{GHz}$) wavelength and tolerances on geometry measurements keep the same order of magnitude, making the degree of accuracy of the simulation decrease.

For such reasons, the most meaningful value to estimate is *expected value* of electrical field strength which provides a good estimation of the real field with an higher level of significance. Due to the uncertainty on the environment geometry model, it can be assumed that the phase between rays incident in one point of the space is a random variable equally distributed in the $[0, 2\pi)$ interval. The expected value of the electric field can be calculated with the solution of the integral:

$$\frac{1}{2\pi} \int\limits_0^{2\pi} \sqrt{h^2 + k^2 - 2kh\cos\theta}\, d\theta$$

In the case of only two incident rays, where h and k are the magnitudes and θ is the phase difference related to the contributes of the two incident rays. Unfortunately this integral has no explicit solution and it can be evaluated only with numerical approximations.

One of the most employed methods to approximate this kind of integral is the *Montecarlo* algorithm which estimates the integral value as a mean of N values ($N \gg 1$) of the integrand function evaluated with a random value of θ. This method is not suitable because a good approximation requires a very large N, so increasing the complexity of the algorithm.

Other less expensive methods, like *Simpson* formula or *spline-based* approximation, can be used too and they are more resource saving if compared to *Montecarlo* algorithm, but since the improvement of such algorithm is a crucial task to make the simulation as fast as possible another solution was adopted.

The suggested solution for this integral is a different kind of approximation and is useful only for this case. The approximation is based on the periodic form of the function to be integrated: it denotes a similarity with a *cosine* shape. Obviously the only cosine is not enough to represent the function, therefore an error function is needed to correctly perform the approximation. It is not necessary to find an optimal approximation of the error function, since it's fundamental just its integral value. A deep analysis on the integral of the error function has given a simple form to represent with good approximation its value.

The final form (not in minimal terms) of the integral approximation is:

$$|h - k| + \frac{2}{\pi}(h + k - |h - k|) + \min(h, k)\frac{k_1}{k_2^{\frac{\max(h,k)}{\min(h,k)}} - k_3}$$

where k_1, k_2, k_3 are free coefficients calculated to fit the approximation with the real integral.

Validation and Calibration of a 3D Ray Tracing Propagation Model for Urban Environment at UMTS Frequencies

Marco Allegretti, **Claudio Lucianaz**, **Riccardo Notarpietro**, and **Giovanni Perona**

Electronic Department, Politecnico di Torino

C.so Duca degli Abruzzi 24, Torino 10129, Italy

Abstract— This work depicts results from outdoor UHF measurement campaigns carried out in dense urban environment. The analysis focuses on the 2 GHz frequency band chosen for the UMTS standard. The optimization of urban micro-cells requires accurate propagation models, but urban structures can present important changes from a region to another which make unuseful even the most complex models. Old cities are characterized by an irregular layer defined by narrow streets and unequal building, while modern towns have a squared structure with parallel and orthogonal streets. Turin city (Italy) presents a combination of both structures.

In order to characterize the EM propagation in such environments a measurement campaign was carried on. The chosen area is a square 3×3 Km centered around the "Politecnico di Torino" university building: the size of the area was chosen in order to include at least one UMTS urban microcell that usually is less than 1 Km in radius. The transmitter was installed on the roof of the university building and measurements were carried out following two different approaches:

1. Omnidirectional measurements with a moving van in order to determine the field coverage around the transmitter. The receiving antenna was mounted on the roof of a van at an height of about 3 meters and inside it was set up an automated measurements chain. The chain was made of a discone antenna, a Spectrum Analyzer controlled via GPIB interface, a PC used as automated logger and a GPS receiver to acquire the exact position for every measurement point. Routes were planned in order to investigate both LOS and non-LOS zone.

2. Directional measurements in order to characterize building scattering. The aim is to point out and to distinguish the presence, at the receiver, of the various terms due to direct, reflected and building scattered field. The study of such phenomena allowed the construction of fine models that discriminate the effects introduced by the different building architectures and streets' shape.

Measurements highlighted canyoning phenomena that establish in dense urban area, were buildings play a very important role as scatterers. The study of the interactions between an electromagnetic wave and buildings, in further analysis could be integrated with the statistical effects on the signal fluctuations (for example due to traffic).

Measurements were then compared with the predictions obtained by a deterministic EM propagation software based on Ray Tracing and a good agreement was found. The same measurements were at last used to calibrate the software prediction model with good final results.

Surface Wave Propagation above a One-dimensional Rough Sea Surface at Grazing Angles

Y. Brelet, **N. Déchamps**, **C. Bourlier**, and **J. Saillard**

IREENA, Université de Nantes, Polytech'Nantes, Rue Christian Pauc
La Chantrerie, BP 50609, 44306 Nantes Cedex 3, France

Abstract— The scattering of electromagnetic waves from a finitely conducting one-dimensional random rough surface at grazing angles is investigated, what, one of many practical interests, concerns wave propagation over a sea surface from a coastal radar (Fig. 1).

Study is firstly done using the conventional small perturbation method (SPM), by mean of the "extinction theorem" [1]. This theory applies to rough surface with small Root-Mean-Square (RMS) heights compare to the incident wavelength. The fields are calculated *on* the surface and the scattered fields in the half-space (vacuum) above the surface. In this paper, the authors present the computation of this asymptotic method with an exact one. The latter is a recent fast rigorous numerical method, Forward-Backward Novel-Spectral-Acceleration (FBNSA) approach [2], with complexity of order $\mathcal{O}(N)$, based on the Method of Moments, and adequate for such a scattering problem since the number of unknowns is of order of 6000 for an incidence angle of 85°.

It is then put forward that the small perturbation method is applicable for moderate angles of incidence (smaller than 80°). On the other hand, it tends to fail for grazing angles in TM polarization, whereas it does not in horizontal polarization (H or TE polarization).

These observations lead to use the extended small perturbative method [3, 4] based on the Green formalism, to take into account complex propagation occuring in TM case, that classical perturbation theory does not include. This extended method is derived in a similar manner of the Zenneck-Sommerfeld solution [5], when the source and/or observation points are located near the surface. The asymptotic theory of Fuks et al. and Ishimaru et al., quoted above, needs to be numerically tested, and possibly improved. This theory was derived for the coherent and incoherent scattered fields. The authors propose the derivation of the exact fields *on* the rough surface and scattered fields in the upper-half space with both analytical and rigorous methods mentionned above.

Therefore, the aim of the final paper is to present comparisons of the fields *on* the surface and in the upper-half space, derived from the extended SPM theory, with the fast rigorous FB-NSA, to verify if the Zenneck surface wave may occur at the V polarization for a rough surface, when the radar is closed to the surface with frequency ranges $f \in [1; 500]\,\text{MHz}$.
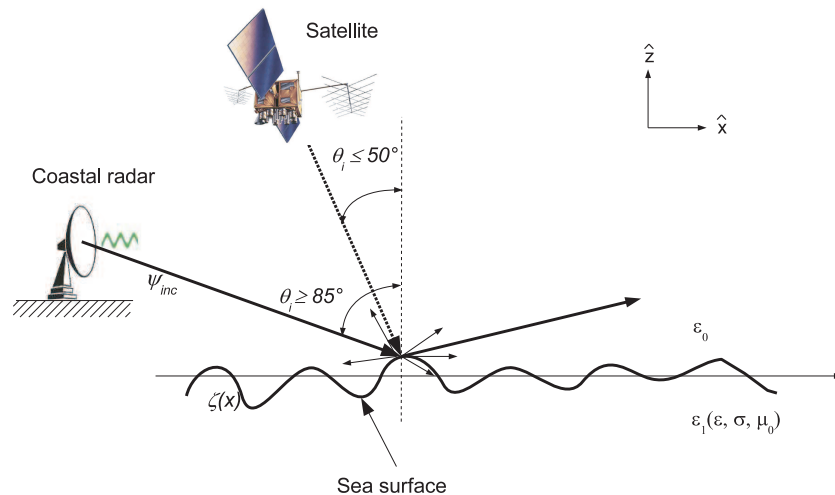
Figure 1: Incident field from a coastal radar onto a conducting medium with real permittivity ϵ, conductivity σ and permeability μ_0. Conducting medium is bounded by rough surface given by the height $z = \zeta(x)$.

REFERENCES

1. Pattanayak, D. N. and E. Wolf, "General form and a new interpretation of the Ewald-Oseen extinction theorem," *Opt. Commun.*, Vol. 6, 217–220, 1972.
2. Chou, H.-T., "A novel acceleration algorithm for the computation of scattering from rough surfaces with the forward-backward method," *Radio Science*, Vol. 33, No. 5, 1277–1287, Sept. 1998.
3. Bass, F. G. and I. M. Fuks, "Wave scattering from statistically rough surfaces," *Pergamon*, Oxford, 1979.
4. Ishimaru, A., J. D. Rockway, Y. Kuga, and S.-W. Lee, "Sommerfeld and Zenneck wave propagation for a finitely conducting one-dimensional rough surface," *IEEE Transactions on Antennas and Propagation*, Vol. 48, No. 9, 1475–1484, 2000.
5. Sommerfeld, A. N., "Propagation of waves in wireless telegraphy," *Ann. Phys.*, Leipzig, Vol. 81, 665–737, 1919.

Simulations of Magnetically Tunable Ferrite/Dielectric/Wire Negative Index Composites

F. J. Rachford[1], D. N. Armstead[2], Vincent Harris[3], and Carmine Vittoria[3]

[1]Naval Research Laboratory, 4555 Overlook Ave SW, Washington, DC 20375, USA
[2]The College of Wooster, Department of Physics, 308 E. University St., Woster, Ohio 44691, USA
[3]Electrical and Computer Engineering Department, Northeastern University, 440 Dana Research Center
360 Huntington Ave., Boston, MA 02115-5000, USA

Abstract— We have performed extensive finite difference time domain (FDTD) simulations to design ferrite based negative index of refraction (NIM) composites. Our simulations center on the use of Barium M type ferrite with in-plane anisotropy to provide the magnetically tunable permeability. A wire grid is employed to provide negative permittivity. The ferrite and wire grid interact to provide both **negative** and **positive** index of refraction transmission peaks in the vicinity of the BaM resonance with several GHz tunable index at Q-band frequencies. We find that the wires and the ferrite must be spatially separated by a low loss dielectric (Mylar). The ferrite and dielectric lamina are paired with combined thickness equal to the square wire grid lattice distance. We assume the presence of a in plane orienting magnetic field. Working with thin planar oriented ferrite lamina implies that the composites will have a negative index in only one direction of propagation. Notwithstanding the extreme anisotropy in the index of refraction of the composite, negative refraction is seen at the composite air interface allowing the construction of a focusing concave lens with magnetically tunable focal length.

Theoretical and Real Absorption of High-frequency Electromagnetic Energy in Mouse Animal Model

J. Barcal[1], **V. Žalud**[1], **F. Vožeh**[1], and **J. Vrba**[2]

[1]Department of Pathophysiology, Faculty of Medicine Pilsen
Charles University in Prague, Czech Republic
[2]Department of Electromagnetic Field, Faculty of Electrical Engineering
Czech Technical University in Prague, Czech Republic

Abstract— High frequency electromagnetic field (HF EMF) became a common part of our environment because it is produced by many artificial sources as radars, transmitters and especially cellular (mobile) phones. Considering a possible harmful effect of it the term "electromagnetic smog" is often used for this situation. Among the sources mentioned, first of all the number of mobile phones is rapidly rising (10 million devices was in the Czech Republic in 2005!) and during a call the source of radiation is close to the head. That is why there is a question of possible negative effects of HF EMF on a human body, especially on the brain. HF EMF can influence tissues by both thermal and nonthermal effects. While the thermal effect is relatively well known, the nonthermal effects are still discussed and remain unclear. In the presenting study we demonstrate a possible methods for theoretical and real measurement of HF EMF absorption using 900 MHz generator.

Experimental animals were exposed to HF EMF with frequency of 900 MHz. Output power of the HF EMFgenerator after amplifying was aproximately 10 W. Mice were placed into a plastic box just before the orifice of the waveguide. Control mice were kept in analogous conditions without the HF EMF. In the first phase model experiments which are able to detect SAR (**S**pecific **A**bsorption **R**ate) were performed. This value shows a absorption dose of radiation in the animal tissue. 10 W output power is radiated as equal quanta from the area cca 600 cm^2 of waveguide. In the distance 0.3 m from the orifice is practically impossible to measure SAR directly and only an estimate (from the gradient of field) suggest the whole-body exposure which correspond to the triple power of classical GSM.

In the second part a computerized modeling of electromagnetic field absorption in the animal body was created. To estimate SAR in experimental animals we have done basic 3D calculation of electromagnetic energy distribution in a simplified dielectric model of an adult mouse. The model consists of a homogenous lossy dielectric material mimicking muscle tissue and has shape of a cylinder (radius 3 cm and high 9 cm terminated to cone) with dielectric properties $e_r = 54$, conductivity $s = 0.8$ S/m, density $r = 1000$ kg/m^3. The calculations were done with the aid of 3D electromagnetic field simulator SEMCAD which used FDTD (**F**inite **D**ifferent **T**ime **D**omain). The method is based on the fact that original continuous function is replaced by the set of discrete function's values. Maxwell's equations are discretized using a 2nd order finite-difference approximation both in space and in time in an equidistantly spaced mesh. Several simulations for different positions of mice were done. Input power during simulations was normalized to 1 W.

Calculations of SAR performed in connection with the simulation of absorption electromagnetic energy by experimental animals using the arteficial dielectric model showed the dependence of the absorption on the real topical position of the mouse against the waveguide and was in the range of 0.05 to 1.44 mW/g.

The complex knowledge resulting from these experiments is not only a contribution to the store of basic neuropathophysiological information but will be also useful for clinical neuropathology with possible consequences for the public health prevention.

Microwave Applicator for Treatment of Atherosclerosis

Kateřina Novotná and Jan Vrba

Department of Electromagnetic Field, Czech Technical University in Prague
Technická 2, 166 27 Prague 6, Czech Republic

Abstract— One of prospective domains of microwave thermotherapy is microwave angioplastic for treatment of atherosclerosis. Due to dysfunction of endothelium a sedimentation of cholesterol on a blood vessel wall can happen. This evokes its sequential closing. Basic principle of microwave angioplastic is, that heating gained by microwave energy irradiated into artery by microwave applicator, enables safe clear out of atherosclerotic plates in the wall of vessel.

Methods: This paper describes the design of special applicator for microwave angioplastic. As the most acceptable structure to create intracavitary applicator, coaxial quarter wave monopole, was chosen. The applicator in our model was inserted into vein with blood and surrounded by phantom of muscular tissue. First goal was to obtain good impedance matching between generator and microwave applicator. Then we studied the distribution of absorbed power (SAR) along the applicator. For the applicator working at 2,45 GHz there was maximum of SAR at point of termination of outer conductor.

Results: The function of the microwave applicator was experimentally evaluated by measurement of reflection coefficient. This tested applicator had good impedance matching, less than -20 dB. Then the distribution of the temperature along the applicator was measured with IR camera. Described applicator was placed in to the phantom of muscular tissue and exposed by 50 W during 1 minute. The temperature grew to 47°C (Fig. 1).
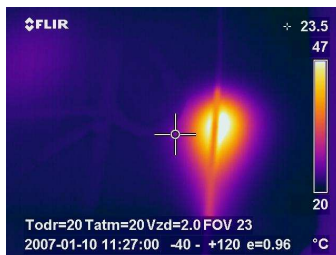
Figure 1: The distribution of the temperature along the applicator.

Conclusion: This paper describes only technical solution to design the intracavitary applicator for microwave angioplastic. Into the future we plan the cooperation with medical doctors, who will provide us the medical information. Main goal of this project is to determine the optimal temperature for different stadium of this illness.

REFERENCES

1. Novotná, K., "Intracavitary applicator for microwave angioplastic (in Czech)," Diploma thesis, Prague, 2007.
2. Vrba, J., "Medical application of microwave thermotherapy (in Czech)," Publishing by ČVUT, Prague, 2003.

A Fat Dipole Antenna for Spark Switched LC Oscillator

Sang Heun Lee[1], **Young Joong Yoon**[1], **Hoon Heo**[2], **Woosang Lee**[3], **and Dowon Choi**[3]

[1]Yonsei University, Korea
[2]Pohang Accelerator Laboratory, Korea
[3]Agency for Defense Development, Korea

Abstract— Spark switched LC oscillator (LCO) is used to generate damped sinusoidal signal which has wideband width. Specially, some high power wideband systems use LCO because spark switched LCO using gas or insulating oil can radiate high power microwave without self-breakdown. Recently, there are many researches of the equivalent circuit modeling and the various characteristics of LCO, such as high repetition rate, fast recovery time, low spark gap loss and so on. On the other hand, the fat dipole antenna which is attached to LCO is not significantly mentioned. Although the length of dipole affects operating frequency and field strength, a dipole antenna is just regarded as $50\,\Omega$ or $100\,\Omega$ load in the equivalent circuit model of LCO [1, 2]. In many case, dipole length is not considered to determine the operating frequency [1, 2].

Therefore, received field of LCO is analyzed according to the variation of a dipole length which is shown in Fig. 1. The operating frequency is 430 MHz when x is 0 mm and it gradually lower until 300 MHz when x is 150 mm. This experimental result and analysis will be useful to design of LCO which uses a fat dipole because the variation of the dipole length changes the operating frequency of LCO.
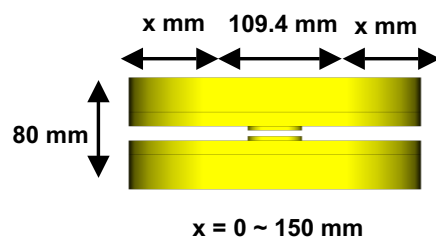
Figure 1: The designed LCO and dipole.

REFERENCES

1. Rinehart, L. F., J. F. Aurand, J. M. Lundstrom, C. A. Frost, M. T. Buttram, P. E. Patterson, and W. R. Crowe, "Development of UHF spark-switched L-C oscillators," *Pulsed Power Conference*, 1993. *Digest of Technical Papers. Ninth IEEE International*, Vol. 2, 534–537, 21–23 June, 1993.
2. Moran, S. L., "High repetition rate LC oscillator," *IEEE Transaction on Electron Devices*, Vol. 26, Issue 10, 1524–1527, 1979.

Frequency Responses of Reconfigurable Frequency Selective Surfaces Using Square Aperture with Loading

Kihun Chang and Young Joong Yoon

Yonsei University, Korea

Abstract— In this paper, frequency responses of reconfigurable frequency selective surface (RFSS) with squared aperture with loading are introduced. The electromagnetic properties of the frequency selective surface (FSS) can be changed by applying a dc bias to the substrate. The proposed structure can be designed to switch between a reflector and a transparent surface at resonance, while the reported structures provides the FSS tuned to higher or lower frequencies.

We discuss square aperture with loading, which can be treated as one prototype of frequency selective surfaces. Secondly we discuss the transmission and reflection curves in RFSS slabs, which are composed of substrate with a symmetric FSS unit cell and PIN diodes. Equivalent circuit in the structure is investigated by analyzing transmission and reflection spectra. Measurements on RFSS are compared with numerical calculation, based on the scattering matrix formalism. The origin of experimentally observed frequency responses will be scrutinized.

ACKNOWLEDGMENT

REFERENCES

1. Munk, B. A., *Frequency Selective Surfaces: Theory and Design*, Wiley, New York, 2000.
2. Bossard, J. A., D. H. Werner, T. S. Mayer, and R. P. Drupp, "A novel design methodology for reconfigurable frequency selective surfaces using genetic algorithms," *IEEE Transaction on Antennas and Propagation*, Vol. 53, No. 4, 1390–1400, April 2005.

2D Quasistatic TLM Field Solver for High Speed PCB Design

Caner Altınbaşak[1] and Lale Tükenmez Ergene[2]

[1]The Scientific & Technological Research Council of Turkey (TUBITAK), Marmara Research Center
Institute of Informatics, Kocaeli, Turkey
[2]Istanbul Technical University, Institute of Informatics, Istanbul, Turkey

Abstract— Modern computer communication busses like PCI-Express or Fibre Channel have rise and fall times nearly 100 ps. Nowadays, increasing speed in computer technology creates new challenges for designers, and the tools they use to design, verify and debug the systems. Generally designers follow general high speed design rules, built up a prototype, make measurements and redesign if necessary.

But short on the shelf cycles of the commercial market forces the industry to speed up design process. Redesigning may cost much and cause the product to be delayed for the production for months. Nowadays field solvers play a crucial role in high speed interconnect design.

In this work, a traditional differential mode serial communication line is chosen for the analysis. 2D Quasistatic TLM algorithm is developed to solve electromagnetic field distribution within PCB stack up. The verification of the results is achieved by using a commercial tool (SI8000 Quick Solver from Polar Instruments) which uses boundary elements method.

Transmission Line Modeling provides a conceptual model which produces a time domain numerical technique for solving networks and fields [1]. To calculate the field distribution in quasistatic state, we will assume sinusoidal source or harmonic fields.

Each node is connected to other four nodes and the circuit (or field) equations must be used to calculate the E value of the neighboring node. There is no time-stepping in this procedure. Field values are extracted directly. Each node builds up five equations: four for neighboring nodes, one for the stub node. The known values are the field values at the surface of the conductors. Height of the PCB is divided into 50 nodes. Width is divided into 100. There is one equation for each node. So the matrix size is 5000×5000. However, as each line has only four elements, using sparse matrix techniques our memory requirement reduces to 20.000 elements, not $5000 \times 5000 = 25.000.000$ elements. A very sparse band matrix with three bands is constructed using these equations. Field value of each node is extracted by solving this matrix. Problem setup consists a broadside coupled stripline PCB. In the first experiment both IO lines are fed with sinusoidal signals in even mode. Then the same procedure is applied for the odd mode.

ACKNOWLEDGMENT

REFERENCES

1. Johns, P. B., "The art of modelling," *IEE Transactions on Electronics and Power*, No. 8, 565–569, 25, 1979.
2. Lindenmeier, S. and P. Russer, "Design of planar circuit structures with an efficient magnetostatic-field solver," *IEEE Transactions on Microwave Theory and Techniques*, Vol. 45, No. 12, December 1997.
3. Christopoulos, C., *The Transmission-line Modelling Method*, IEEE Press, 1995.

An Hybrid Steepest Descent Fast Multipole Method for the Scattering of Electromagnetic Waves by Dielectric Rough Surfaces

Cihan Tuzcu[1], Lale Tükenmez Ergene[1], and Yasemin Altuncu[2]

[1]Institute of Informatics, Istanbul Technical University, Istanbul, Turkey
[2]Electrical and Electronics Engineering Faculty, Istanbul Technical University
Istanbul, Turkey

Abstract— Analysis of electromagnetic scattering by rough surfaces constitutes an important and interesting class of problems in electromagnetic theory due to its potential applications in modeling of ground wave propagation, remote sensing of geophysical terrains such as snow, soil and vegetation etc. Surface based integral equation methods have been widely used in the solution of such problems. One of the main problems is the application of the integral equation methods is that it requires heavy computational work and one has to develop new approaches with reduced computational cost. Steepest Descent Fast Multipole Method is one of the effective methods in this direction and it has been applied to several complex problems. The computational cost can be also reduced by direct methods with high performance and massively parallel codes.

The main objective of this paper is to give a hybrid method which combines the Steepest Descent Fast Multipole Method and Buried Object Approach [1] for the scattering of electromagnetic waves from the dielectric rough surfaces. In the Buried Object Approach the irregularities of the rough surface are assumed to be as buried objects in a two half-space media with planar interface which allows us to formulate the problem as a scattering problem related to cylindrical bodies of arbitrary cross sections. Through the Green's function of the two half spaces medium where the irregularities are buried, the problem is reduced to the solution of a Fredholm integral equation which is solved via an application of Method of Moments (MoM) by reducing it to a linear system of equations. The computational cost of the present method is directly proportional to the number of irregularities of the surface and their sizes. As a result the method is very effective for surfaces having a localized roughness, arbitrary rms height and slope. In the calculation of the Green's function we adopt the Steepest Descent Fast Multipole Method to the present problem [2].The method permits us to obtain both the near and far field expressions of the scattered wave in the half-spaces above and below the surface. We have shown that the results of the method match with those obtained through the existing ones.

ACKNOWLEDGMENT

REFERENCES

1. Altuncu, Y., A. Yapar, and I. Akduman, "On the scattering of electromagnetic waves by bodies buried in a half-space with locally rough interface," *IEEE Transactions on Geoscience and Remote Sensing*, Vol. 44, No. 6, 1435–1443, Jun. 2006.
2. Hu, B. and W. C. Chew, "Fast inhomogeneous plane wave algorithm for electromagnetic solutions in layered medium structures: two-dimensional case," *Radio Science*, Vol. 35, 31–43, Jan. 2000.

Electromagnetic Fundamentals Revisited: An Overview

Subal Kar[1] and M. Nakajima[2]

[1]University of Calcutta, India
[2]University of Kyoto, Japan

Abstract— Does the electromagnetic field propagate as a consequence of time differentiation of physical quantity? Faraday's experiment says so. If this conventional notion is followed, then we have the paradox associated with radiation of e.m energy from a dipole antenna in terms of Poynting vector (usually done on the basis of current element concept!).

However, if we assume that the electric field should me moved first (i.e., charge is the fundamental entity giving rise to the field) in order to excite e.m waves then it may be shown that propagation of e.m wave may take place as a consequence of time integration of physical quantity. On the basis of this concept a sampled-field analysis technique introduced is capable of explaining e.m phenomena from a more fundamental view point. We have established that a generalized plane wave solution is possible for e.m field, irrespective of the field being static or dynamic. Following this approach, we could resolve the paradox of antenna radiation problem need to be addressed on the basis of Poynting vector.

Electromagnetic radiation from antenna is conventionally derived from current flowing through the conductor. However, if e.m radiation from, say, a dipole antenna is to be treated in terms of Poynting vector then as $E_t = 0$ on the conductor surface, the normal component $\vec{E}x\vec{H}$, representing e.m power from the antenna, is zero — thus no radiation can emerge out of the conductor surface of dipole antenna (!) and hence the paradox.

In our model, we consider a plane e.m. wave: $\vec{E}^i = \bar{\bar{E}}^i e^{-j\vec{k}_i \cdot \vec{r}}$, $\vec{H}^i = (k^i/\omega\mu) \cdot \vec{E}^i$ is incident on a plane conductor whose surface lies on the z and x coordinates, the normal of the plane being oriented in the y direction. For the case of TE wave with $\bar{\bar{E}}^i = \hat{x}\bar{E}_x$, we can derive the Poynting vector over the surface of the plane conductor as:

$$\frac{1}{2}\text{Re}(\vec{E}x\vec{H}^*) = \frac{1}{2}\text{Re}(\bar{\bar{E}}^i x\bar{\bar{H}}^{i*}) + \frac{1}{2}\text{Re}(\bar{\bar{E}}^r x\bar{\bar{H}}^{r*}) + \frac{1}{2}\text{Re}(\bar{\bar{E}}^i x\bar{\bar{H}}^{r*} + \bar{\bar{E}}^r x\bar{\bar{H}}^{i*})\cos 2k_y y$$
$$= \hat{z}2Re(\bar{E}_x\bar{H}_y^*)\sin^2 k_y y \tag{1}$$

where the superscripts i and r represent the incident and reflected terms, respectively.

On the basis of this equation the Poynting vector may be interpreted in two ways:

1) Analytical view: The first two terms in the first row on right hand side of Eq. (1) expresses the Poynting vectors for the incident and reflected waves. In this view, the interference term (i.e., the third term on right hand side in the same row) must be taken into account. However, the interference term vanishes, if it is integrated throughout the space over the conductor, on account of the orthogonality of plane waves.
2) Synthetic view: The three terms can be summed up to be a single term, as is written in the last row. This represents energy flow in parallel with the surface of the plane conductor. In the direction normal to the surface, there are energy flows back and forth which produces a standing wave represented by $\sin^2 k_y y$. Standing wave normal to the plane conductor conveys no net energy in the direction normal to the conductor surface.

Solution to the Antenna problem: With the aid of this model, the paradox of the radiation from half wave antenna may be resolved as follows.

The conventional mode of calculation of the Poynting vector may belong to the synthetic view. In this sense, the calculated Poynting vector did not give us the incident and reflected powers to and from the antenna respectively, so that there is no net power flow into or out of the antenna.

However, according to the analytical point of view, which is based on our analysis, the incident and reflected Poynting vectors are separated. We are then led to the interpretation that the incident wave starts from the signal source and excite current in the antenna conductor. While the radiated wave is being caused by the reflected wave. Along the antenna conductor, these two waves are superposed and the resultant Poynting vector becomes parallel to the conductor surface. In the usual observation procedure, these two waves cannot be distinguished. If a sensor such as a direction coupler is created, the exciting wave and emitted wave can be observed separately.

Calculation of GTD/UTD Reflection Points over Parametric Surfaces Using the Particle Swarm Optimizacion

A. Rubio, **O. Gutierrez**, **F. Saez de Adana**, **and M. F. Cátedra**

Departamento de Ciencias de la Computación, Universidad de Alcalá

28806, Alcalá de Henares, Spain

Abstract— A new method to find reflection points on parametric surfaces is presented in this communication. The technique uses the Particle Swarm Optimization to perform the minimization of the path associates with the computation of the reflection points. The points are referred to the parametric coordinates of the surface and a cost function, based on the Snell's Law and the Fermat's Principle, is applied to find the best position. The technique is applied to the computation of the reflection points of the Uniform Theory of Diffraction (GTD/UTD) and it is an alternative to another minimization methods like the Conjugate Gradient, and can be applied to cases where not good convergence is present.

In complex environments, the principal difficulty of the GTD/UTD is the ray-tracing calculation, especially when complex structures with arbitrary shape are analyzed. One of the tasks in the raytracing process is to determine where the rays are reflected or diffracted. These critical points can be calculated using analytical and close expressions when the scene is modeled by flat surfaces. However, for arbitrary curved surfaces, modeled by parametric surfaces, minimization techniques, such as the Conjugate Gradient, must be used. This method obtains good results for convex surfaces, where no local minimums are present. On the other hand, convergence problems can appear for concave surfaces. An alternative technique, based on the Particle Swamp Optimization (PSO), is presented in this communication. The PSO avoids the local minimum, therefore both convex or concave surfaces can be analyzed with the same accuracy.

PSO is an optimizer based on an evolutionary model used to solve engineering problems. It is based in the behavior of a swarm of bees in the search of the biggest flowers concentration. The algorithm defines a number of particles or agents into the solution space as starting solution. After that, each particle moves, randomly, over the space, and in each iteration every particle records its best position (pbest). Also the best position of all the particles is stored (gbest). The application of this algorithm to the computation of the reflection points consists in using a cost function which takes into account the two conditions that the reflection ray must accomplish: the Fermat's principle which says that the distance of the reflected path between the transmitter and the receiver must be minimum and the Snell's law.

Some results have been obtained which prove the accuracy of the method and its advantages with respect to other approaches.

Dielectric Properties of Ore Minerals in Microwave Range

V. V. Tikhonov[1], D. A. Boyarskii[1], and O. N. Polyakova[2]

[1]Earths Exploration from Space Department, Space Research Institute Russian Academy of Sciences
Profsojuznaya, 84/32, Moscow 117997, Russia
[2]Department of Physics, Moscow State Pedagogical University
M. Pirogovskaya, 29, Moscow 119992, GSP-2, Russia

Abstract— Dielectric characteristics of many natural minerals are poorly investigated. The lack of such data poses a problem for modeling the interaction of electromagnetic radiation with many media, such as ground, soils and rocks. This results in significant difficulties in the interpretation of radiometry, radar, subsurface sensing and dielectric spectroscopy data.

Microwave dielectric properties of ore minerals still remain virtually uninvestigated due to considerable technical problems. No data on dielectric properties of such minerals are reported in the literature.

A technique to define dielectric properties of ore minerals is discussed. Using this technique, dielectric characteristics of some minerals in a range of 77–300 GHz are obtained.

The real and imaginary parts of complex dielectric constant of a substance cannot be measured directly and can be derived only from measurements of other parameters (for instance, reflection and transmittance coefficients) through application of a corresponding theory.

Spectral measurements of reflection and transmittance coefficients of plane-parallel samples of the minerals were conducted at a test board at normal radiation incidence. Measurements of reflection and transmittance coefficients were carried out using a carcinotron spectrometer. The spectrometer had a generating unit (with highly-stabilized electronic feed), a receiver unit (optophone and synchronous detector), and also a measuring quasi-optical line.

The real and imaginary parts of complex dielectric constant of a mineral were determined by solving a system of equations for reflection and transmittance coefficients of the multi-layer absorbing film placed between two dielectric media. This system of equations did not allow for an analytical solution and demanded numerical solution using corresponding algorithms and computer software. The problem was solved by minimization of the criterion function. The criterion function was square standard deviation of the theoretical dependence of absorption in a layer from the experimental one in the wave interval where dielectric constant could be considered constant. An algorithm using Rosenbrock method was developed for minimization of the criterion function. This method is a typical method of search with restrictions where minimization directions are completely defined on the basis of consecutive calculations of the criterion function.

In the work, the results of spectral measurements of reflection and transmittance coefficients of plane-parallel samples of some ore minerals (magnetite, chalcopyrite, sphalerite, etc.), in microwave range are presented. On the basis of these dependences, values of real and imaginary parts of dielectric permittivities of the studied minerals in a range of 77–300 GHz are calculated. The results of the calculations are approximated by smooth functions of radiation frequency. The obtained formulas can be used to calculate complex dielectric constant or complex refraction coefficient of ore minerals in a range of 77–300 GHz.

Patch Antenna at Frequency $f = 2.35$ GHz for Telecommunications Applications

K. ELkinani[1], **S. Bri**[1], **A. Nakheli**[1], **O. Benzaim**[2], **and A. Mamouni**[2]

[1]Equipe Hyperfréquences et Matériaux, ESTM, B. P. 3103, Meknès, Maroc
[2]Institut d'Electronique, de la Microélectronique et de Nanotechnologie, UMR CNRS 8520
IEMN, Cité Scientifique, Avenue Poincaré, B. P. 60069 59652, Villeneuve d'Ascq Cedex, France

Abstract— This paper analyzes the effects of electromagnetic radiation from a cellular phone on the head. Various antenna designs were created and analyzed. Special consideration was taken to create an antenna with high efficiency and optimum radiation characteristics in frequency $f = 2.35$ GHz. The antenna was placed next to human head materials and specific absorption rates were calculated. Tests were performed at various distances from the material for analysis and evaluation of the fields. Simulations on the antenna were done on Ansofts Ensemble software. The application of the antenna next to the head and the creation of the head model itself were done on Ansofts High Frequency Structure Simulator (HFSS). The antenna was built and tested on a network analyzer to obtain near field. Mathematical models were used in all designs.

REFERENCES

1. Abd-Alhameed, R. A., K. Khalil, P. S. Excell, and C. H. See, "Simulation and measurement of broadband microstrip patch antenna for 3G wireless communications," The Institute of Electrical Engineers, Printed end Published by the IEE, Michael Faraday House, Six Hiil Wav, Steveneage SG 1 2AY, 2003.

2. Covert, L. and J. Lin, "Simulation and measurement of a heatsink antenna: A dual-function structure," *IEEE Transactions on Antennas and Propagation*, Vol. 54, No. 4, April 2006.

3. Ollikainen, J., O. Kivekäs, A. Toropainen, and P. Vainikainen, "Internal dual band patch antenna for mobile phones," *2000 European Space Agency (ESA), Proceedings of the AP2000 Millennium Conference on Antennas & Propagation*, Davos, Switzerland, 9–14 April, 2000.

Electroplating Uniformity Estimation Using Electromagnetic Analysis

Han Kim

SAMSUNG Electro-Mechanics, Korea

Abstract— As integrated circuit miniaturizes, the manufacturing process of package substrates have become more fastidious to be handled. In particular, the electroplating uniformity control is more difficult because of its inaccuracy estimation.

In generally, the simulation approach for electroplating of package substrate is based on an electrochemical theory. There are some calculation methods and commercial simulation tools using electrochemical analysis for the estimation of electroplating uniformity. However, the typical electrochemical analysis is inadequate for the estimation of electroplating uniformity at PCB (printed circuit board) because it is not included the analysis of bus lines at PCB panel.

In this paper we propose a novel simulation approach using electromagnetic analysis for the estimation of electroplating uniformity. This approach is based on the calculation of current distribution at PCB panel. The current distribution is calculated by using modified material properties at the electroplating bath and the plating uniformity can be represented by using this current distribution.

To verify this proposed approach, we calculated electroplating uniformity at PCB panel by using commercial electromagnetic analysis program and our program for estimation of electroplating uniformity. Both simulation results are comparable with measurement one as shown in Fig. 2–4. The improvement of the electroplating uniformity can be achieved by using this proposed method.
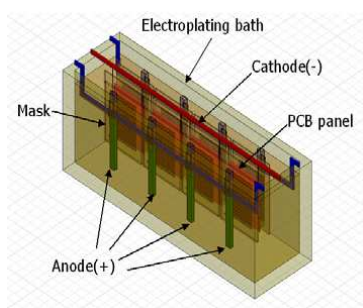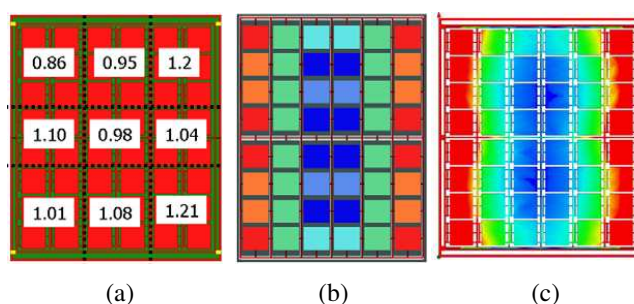
Figure 1: Electroplating bath.

Figure 2: Electroplating uniformity (a) measurement result (b) simulation(commercial program) (c) simulation (our program).

REFERENCES

1. Kim, H. and C.-H. Ahn, "Fast inductance extraction of microstrip lines using adaptive PEEC grid," *Microwave Conference, APMC 2002*, Vol. 1, 81–84, Nov. 2002.

Progress of Mobile Natural Gas Pipeline Leak Detector Based on Near-infrared Diode Laser Absorption Spectroscopy

Lei Wang, **Xiaoming Gao**, **Tu Tan**, **Baixiang Li**, **and Weijun Zhang**

Laboratory of Environmental Spectroscopy, Anhui Institute of Optics & Fine Mechanic
Chinese Academy of Sciences, Hefei 230031, China

Abstract— Natural gas is a cleanly energy source, which has very high benefit at environmental protection and improving people health as a substitute of coal. China government will encourage the using of natural gas, decrease the dependence on coal and petroleum, but the distribution of china natural gas is unbalanced. To solve the problem, china government has built a natural gas pipeline from west to east in china, and will build five transverse and two longitudinal main natural gas nets covering whole china. For these long transport pipelines, the leakage of the natural gas is unavoidable. Detecting leakage sources is a very laborious task.

We have developed a portable natural gas pipeline leak remote detector based on near infrared diode laser absorption spectroscopy. Based on the groundwork, we are developing a mobile natural gas pipeline leak remote detector. The reflected scattering laser was collected by a $\phi114$ lens to focus on a detector, the ratio between first and second harmonic was recorded. A bag filled 0.3% methane mixture gas was set at far away 7 m from the detector. The detector was mounted on a simulated mobile platform. Rotating the platform, the different scanning angle speeds corresponded to different transfer speeds. The laser was scanned across the gas bag come-to-go. The recorded signals at different transfer speeds were showed in Figure 1. We can know that the signals at lower moving speed had small fluctuation, at high moving speed, the fluctuation is large. The fluctuation will be decreased by setting the parameters of the system. In the system, we will realize automatic storage of pipeline leak information using a GPS (Global Positioning Systems) and a CCD camera. The saved information will include methane concentration, the leak position, leak scene and distance from the detector.
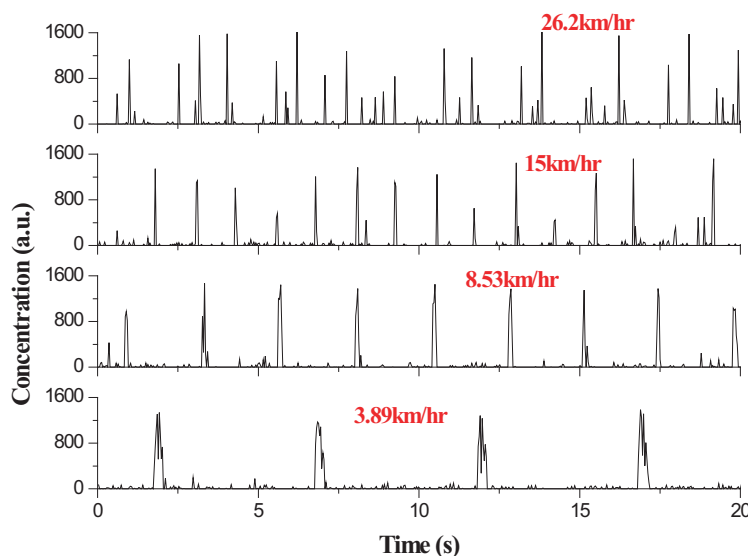

Figure 1: Measured methane concentration at different transfer speed.

Incoherent Broadband Cavity-enhanced Absorption Spectroscopy Based on Light-emitting Diodes

Tao Wu[1], **Weijun Zhang**[1], **Weidong Chen**[2], **Weixiong Zhao**[1], **and Xiaoming Gao**[1]

[1]Anhui Institute of Optics & Fine Mechanics, Chinese Academy Sciences, Hefei 230031, China
[2]MREID, Université du Littoral, 145 Av. Maurice Schumann, Dunkerque 59140, France

Abstract— A compact incoherent broadband cavity-enhanced absorption spectroscopy (IB-BCEAS) system has been established at visible wavelengths using a high powered blue light emitting diode (LED). The LED light was coupled into a 92.5 cm long high finesse cavity that composing of two 30 mm diameter spherical mirrors (1.0 m radius of curvature) with reflectivity of ~ 0.993. The light leaked out of the cavity was collected by a compact CCD spectrometer (HR 2000). The IBBCEAS spectrum of NO_2 has been recorded at 455 μm.

The reflectivity of the mirrors was measured as a function of wavelength using standard concentrations of NO_2 and further confirmed by absorption of O_2-O_2 collisional pair. The minimum detectable concentration of NO_2 is estimated to be 7 ppbv for a 60 s averaging period in the system.
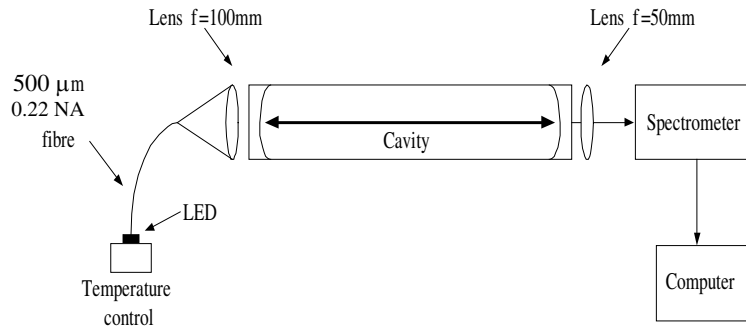
Figure 1: Experimental set-up for incoherent broadband cavity-enhanced absorption instrument.

REFERENCES

1. Langridge, J. M., S. M. Ball, and R. L. Jones, *Analyst*, Vol. 131, 916–922, 2006.